Available online at www.sciencedirect.com

ScienceDirect

journal homepage: www.elsevier.com/locate/he

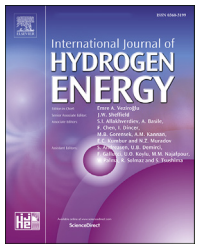

Full-cell hydride-based solid-state Li batteries for energy storage

Michel Latroche [a,*], *Didier Blanchard* [b], *Fermín Cuevas* [a], *Abdelouahab El Kharbachi* [c], *Bjørn C. Hauback* [c], *Torben R. Jensen* [d], *Petra E. de Jongh* [e], *Sangryun Kim* [f], *Nazia S. Nazer* [c], *Peter Ngene* [e], *Shin-ichi Orimo* [f,g], *Dorthe B. Ravnsbæk* [h], *Volodymyr A. Yartys* [c]

[a] *Université Paris Est, Institut de Chimie et des Matériaux Paris Est, ICMPE, CNRS-UPEC, F- 94320 Thiais, France*
[b] *Department of Energy Conversion and Storage, Technical University of Denmark, Frederiksborgvej 399, P.O. Box 49, DK-4000 Roskilde, Denmark*
[c] *Institute for Energy Technology (IFE), P.O. Box 40, NO-2027 Kjeller, Norway*
[d] *INANO and Department of Chemistry, Aarhus University, Langelandsgade 140, DK-8000 Aarhus, Denmark*
[e] *Inorganic Chemistry and Catalysis, Debye Institute for Nanomaterials Science, Utrecht University, Utrecht, The Netherlands*
[f] *Institute for Materials Research, Tohoku University, 980-8577 Sendai, Japan*
[g] *WPI-Advanced Institute for Materials Research, Tohoku University, 980-8577 Sendai, Japan*
[h] *Department of Physics, Chemistry and Pharmacy, University of Southern Denmark, Campusvej 55, 5230 Odense M, Denmark*

ARTICLE INFO

Article history:
Received 28 September 2018
Received in revised form
21 December 2018
Accepted 24 December 2018
Available online 2 February 2019

Keywords:
Metallic and complex hydrides
Battery
Anode
Electrolyte
Lithium
Operando

ABSTRACT

Metallic and complex hydrides may act as anode and solid electrolytes in next generation of lithium batteries. Based on the conversion reaction with lithium to form LiH, Mg- and Ti-based anode materials have been tested in half-cell configuration with solid electrolytes derived from the hexagonal high temperature modification of the complex hydride $LiBH_4$. These anode materials show large first discharge capacities demonstrating their ability to react with lithium. Reversibility remains more challenging though possible for a few dozen cycles. The work has been extended to full-cell configuration by coupling metallic lithium with positive electrodes such as sulfur or titanium disulfide through complex hydride solid electrolytes. Beside pure $LiBH_4$ which works only above 120 °C, various strategies like substitution, nanoconfinement and sulfide addition have allowed to lower the working temperature around 50 °C. In addition, use of lithium *closo*-boranes has been attempted. These results break new research ground in the field of solid-state lithium batteries. Finally, *operando* and *in-situ* neutron scattering methods applied to full-cells are presented as powerful tools to investigate and understand the reaction mechanisms taking place in working batteries.

* *Corresponding author.*
E-mail address: michel.latroche@icmpe.cnrs.fr (M. Latroche).
https://doi.org/10.1016/j.ijhydene.2018.12.200

Introduction

Dense energy packing is a key issue for future development of renewable energy production and will lead to increasing needs for mass storage. Energy can be stored in many ways, but chemical and electrochemical ones are foreseen as very promising in the future. In that field, hydrogen-based energy storage offers a good alternative to other methods and has been extensively studied in the frame of the IEA-HIA task 32. Beside solid-state storage of gaseous hydrogen with metallic or complex hydrides, electrochemical storage is one of the most advanced commercial applications developed so far, for hydrides with well-known alkaline Ni-Metal Hydrides (NiMH) [1–4]. Recently, a breakthrough was realized by demonstrating that metal or complex hydrides can be also used for lithium-based electrochemical cells either as anodes or electrolytes. Lithium batteries are considered as one of the most advanced technologies for electrochemical energy storage. However, their energy densities are still too low to respond to the highly demanding mass storage and they suffer from serious safety issues, mainly related to the use of organic liquid-based electrolytes. Using hydrides for such batteries can bring smart solutions to those drawbacks as they can be implemented either as high-capacity anodes through a conversion reaction with lithium or/and as high-ionic conductivity solid electrolyte allowing fast lithium transport between both electrodes.

Several review papers [5–7] have been already published on this topic by IEA-HIA task 32 partners but, beyond the materials properties of complex or metallic hydrides, the most important challenge consists of building practical batteries. The present paper focusses on the recent development of half- and full-cells[1] using the combination of solid hydride-based electrolytes and metal hydride anodes that pave the way to future hydride-based efficient electrochemical storage systems, and further expand the concept of Li-ion battery technology. It also addresses the needs for *operando* or *in-situ* characterization of working batteries using penetrating neutron beams to probe reaction mechanisms within the electrochemical cells.

Half-cell configurations combining metal hydride anode and complex hydride electrolyte

$Mg_2FeH_6|LiBH_4|Li$

The complex hydride Mg_2FeH_6 was recently employed as conversion type anode with a solid state $LiBH_4$ electrolyte at 120 °C [8]. This configuration provided a factor-3 increase in the capacity retention compared to the conventional counterpart employing standard liquid electrolyte. The initial columbic efficiency also improved from the use of the solid-state electrolyte by a factor of approx. 2.5. Characterization of the charge-discharge mechanism in the MgH_2 and $LiBH_4$ system showed that it follows the expected conversion reactions according to Eq. (1) [9].

$$Mg_2FeH_6 + 6Li^+ + 6e^- \rightarrow 2\,Mg + Fe + 6LiH \quad (1)$$

However, cyclic voltammetry, galvanostatic intermittent titration and PXD suggested that MgH_2 may form as an intermediate during both charge and discharge [8].

MgH_2+CoO|$LiBH_4$|Li

Ongoing research on MgH_2 shows that the capacity retention can be enhanced by addition of an electrochemically active CoO conversion-type anode to MgH_2 [10]. This approach consisted first to assess the performance of the improved single MgH_2 anode (without any added catalyst) and then after CoO addition in solid-state Li-ion battery configuration using $LiBH_4$ as solid electrolyte at 120 °C. The cycling led to formation of a single-plateau of the $75MgH_2$+25CoO nanocomposite electrode with higher reversibility yield, lowered discharge-charge hysteresis and mitigated kinetic effect. The presence of CoO is clearly contributing to the improvement of the cyclability and reversibility while remaining active and delivering an extra capacity. Reduced diffusion pathways and less polarized electrodes are believed to be at the origin of such beneficial properties, owing to the *in-situ* formation of highly dispersive Co/CoO nanoparticles in the electrode matrix.

$MgH_2|(Li(BH_4)_{0.75}I_{0.25})+(Li_2S)_{0.80}(P_2S_5)_{0.20})|Li$

While using $LiBH_4$ as solid electrolyte, the need for heating at 120 °C to get good ionic conductivities will limit its usage to some applications where the source of heat is accessible at low cost. Tentative to lower the temperature, down to room temperature, of the Li^+ conducting solid-electrolyte in the $MgH_2|LiBH_4|Li$ cell by halide-substitution and further $(Li_2S)_{0.80}(P_2S_5)_{0.20}$ solid electrolyte incorporation has been reported recently by Hauback's group [11]. The study demonstrates a possible improvement (1st cycle almost full reversible capacity) at moderate temperature while the optimization of the configuration is needed.

An apparent increase of the capacity can be seen during recharge. This is may be due to the complexity of the conversion mechanism in a solid-state configuration during the phase separation ($MgH_2 > Mg + 2LiH$), along with the changes in the structural, electronic and surface variations between the (dis) charged states [11]. Only few studies reported on the conversion mechanism in solid-state batteries; one can expect that future works can bring more insights on this type of combination and potential prospects.

Microstructural characteristics (synchrotron radiation powder X-ray diffraction (SRPXD) and transmission electronic microscopy (TEM)) of the MgH_2 powder used in this study are shown in Fig. 1aand b), indicating a well crystalline *tetra*-MgH_2 with reduced grain size (3–7 nm). Particles with sizes in the order of 150 nm can be seen (Fig. 1b), though some larger agglomerates are still present. The calculated *d*-spacings from the spots agree with *tetra*-MgH_2. The solid electrolyte was synthesized by mixing the hexagonal phase $Li(BH_4)_{0.75}I_{0.25}$ with $(Li_2S)_{0.80}(P_2S_5)_{0.20}$ precursor followed by annealing at 240 °C and 20 bar H_2. The final product gives an ionic conductivity of about 10^{-4} S cm^{-1} at room temperature (RT).

[1] In this paper, half-cell signifies a cell made of lithium as counter-electrode facing a "low potential active material" that can be considered as a negative electrode (or anode) while full-cell defines a cell made of lithium (or metallic hydrides) facing a "high potential active material" that can be considered as a positive electrode (or cathode) in a real battery.

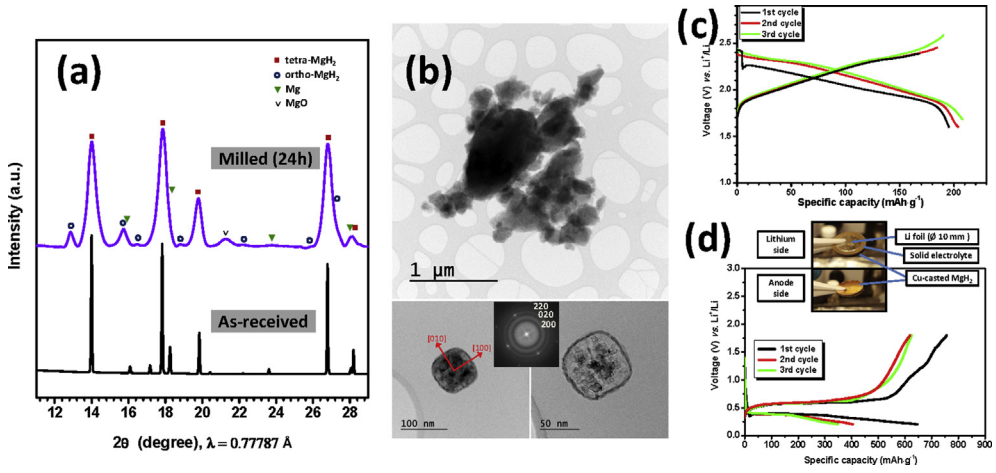

Fig. 1 – PXD patterns (a) and bright field TEM micrographs (b) of the 24h-milled MgH_2 under H_2 atm. (Inset: Fourier transform of the bright field TEM image); RT discharge-charge (3 first cycles, 30 °C, 0.01 mA cm^{-2}) galvanostatic profiles of the standard TiS_2 electrode (c) and MgH_2 tape (d) using the same SE. Inset: two-sided picture of the assembled different layers of the solid-state Li-ion cell [11].

This electrolyte system was tested first with TiS_2 electrode at low applied currents at *RT* in the configuration $TiS_2|Li(BH_4)_{0.75}I_{0.25}+(Li_2S)_{0.75}+(P_2S_5)_{0.25}|Li$ (Fig. 1c). The capacity of the initial discharge corresponds to 89% of the theoretical one with a reversibility yield of around 90%. Up to one Li can be inserted assuming Eq. (2):

$$xLi^+ + xe^- + TiS_2 \rightarrow Li_xTiS_2 \quad (2)$$

The discharge/charge profiles were then recorded for the same cell configuration when TiS_2 electrode is substituted by MgH_2 tape electrode (Fig. 1d) [11]. It presents flat discharge-charge plateaus and low polarization-hysteresis. The obtained discharge capacity reflects only a part of the total active material; most probably the loaded mass is not fully involved in the process. Interestingly, the obtained 1st cycle reversibility exceeds significantly the one obtained with liquid electrolyte for the same MgH_2 tape electrode [12]. The results point to a means of guided cell assembly and possible enhancement at the electrode/electrolyte level and fabrication process.

Full-cell configurations using Li metal anode and complex hydride electrolyte

$Li|LiBH_4+LiCl|S$ or TiS_2

Solid-state Li-S (working voltage = 2.2 V) [13,14] and Li-TiS_2 (working voltage = 2.1 V) [15] employing $LiBH_4$ as solid electrolyte present high performances over repeated discharge-charge cycles. The Li-S battery delivered an initial discharge capacity of 1140 $mAhg^{-1}$ at a rate of 0.05C (C = 1672 mA g^{-1}) at 393 K, which corresponds to 68.2% of the theoretical capacity (1672 $mAhg^{-1}$) [14] (Fig. 2a). In addition, 64.0% of the initial capacity was retained after 45 cycles. In the case of Li-TiS_2 battery cycled at a rate of 0.2C at 393 K, the discharge capacity was 205 $mAhg^{-1}$ (theoretical capacity = 239 $mAhg^{-1}$) in the second cycle, and this value dropped only to 180 $mAhg^{-1}$ after 300 cycles, corresponding to an 87.8% capacity retention [15] (Fig. 2b). A combined experimental and computational analysis revealed that the $Li_2B_{12}H_{12}$ interfacial phase, which displays superior oxidative stability compared to $LiBH_4$, was formed between the TiS_2 cathode and the $LiBH_4$ solid electrolyte, enabling the reversible and stable lithium ion transfer across the interface.

The main challenge of the $LiBH_4$ solid electrolyte is the high phase transition temperature, requiring high temperature operations. In this regard, the substitution of halide ions such as Cl^-, Br^-, and I^- for the BH^- complex anions in $LiBH_4$ significantly lowers its phase transition temperature [16], leading to considerable progress in all-solid-state batteries using $LiBH_4$-based solid electrolytes. When the Cl^--substituted $LiBH_4$ ($Li[BH_4,Cl]$), which displays the phase transition at approx. 345 K, was used as solid electrolyte, solid-state Li-S batteries showed reversible discharge-charge reaction even at 383 K [13] (Fig. 2c). However, the battery using $Li[BH_4,Cl]$ showed worse cyclability compared to that using $LiBH_4$, due to the alleviated electrochemical stability of the solid electrolyte by the Cl^--substitution.

$Li|LiBH_4@SiO_2|S$

Solid-state lithium-sulfur batteries with $LiBH_4@SiO_2$ nanocomposite as electrolyte were also realized by Das et al. [17]. In these $Li|LiBH_4@SiO_2|S+C$ batteries, Li metal on stainless steel current collector is used as negative electrode while the solid-electrolyte is a composite of $LiBH_4$ and ordered mesoporous silica (MCM-41) prepared via melt infiltration under hydrogen pressure [18,19]. The solid electrolyte contained 54 wt% $LiBH_4$ which corresponds to 160% of the pore volume of the silica, allowing the extra $LiBH_4$ to provide a percolating ion pathway between the two electrodes. The S+C electrodes were fabricated by ball-milling mixture of elemental sulfur and conductive carbon (45:55, S:C weight ratio) followed by melt-diffusion at 155 °C to improve the dispersion of sulfur in the carbon matrix [20]. The conductive carbon is a mixture (1:1 wt

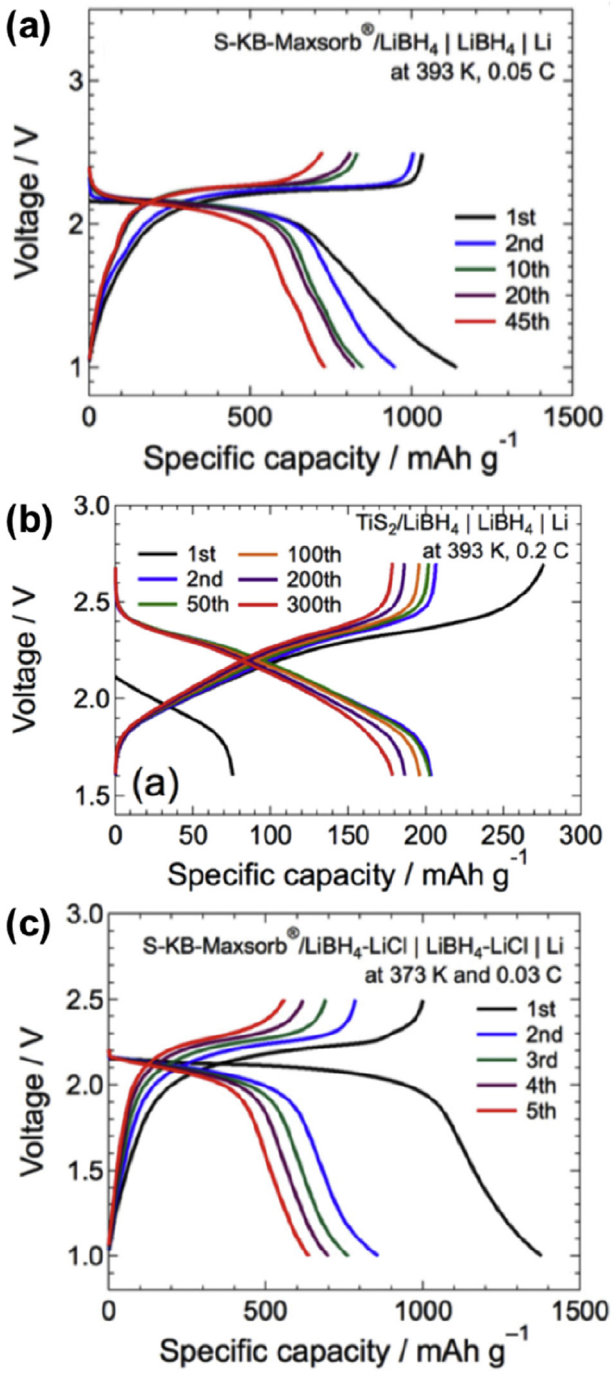

Fig. 2 – All-solid-state batteries using $LiBH_4$-based complex hydride solid electrolytes. Discharge-charge profiles of (a) Li|$LiBH_4$|S [14], (b) Li|$LiBH_4$|TiS_2 [15], and (c) Li|$LiBH_4$+LiCl|S batteries [13].

ratio) of Ketjen Black and activated carbon, a compromise between high electronic conductivity and large surface area, with 10–15 wt% polyvinylidene fluoride (PVDF) added as binder.

The authors showed that the nanoconfined $LiBH_4$ exhibits very good properties as solid electrolyte to be used in lithium-sulfur batteries. They reported a conductivity of 10^{-4} Scm^{-1} at room temperature, three orders of magnitude larger than that of unmodified $LiBH_4$ and investigated the nature of the conduction in $LiBH_4$@SiO_2 nanocomposite by measuring the electronic (t_e), ionic (t_{ion}) and cationic transport numbers (t_+) which are crucial properties for effective electrolytes in battery applications. They showed that the composite has a cationic transport number of 0.96 and negligible electronic conductivity, hence the nanocomposite is close to a pure cationic conductor. The stability of the nanocomposite in contact with lithium metal was investigated by galvanostatic plating-stripping cycles using symmetric Li electrode cells. Only a slight increase (4.5%) in cell resistance was observed in 40 cycles. This is excellent for solid electrolytes, which are known to face challenges, reacting with lithium metal or with maintaining good interfacial contact with electrode materials during cycling.

The solid-state Li-S battery realized with $LiBH_4$@SiO_2 nanocomposite electrolyte showed a very good performance, delivering high capacities, typically 1220 $mAhg^{-1}$ after 40 cycles at moderate temperature (55 °C) and working voltage of 2 V, albeit at a relatively low charge-discharge rates (0.03 *C*). Except for the first cycle, the cyclic voltammogram of a solid-sate Li-S battery (Fig. 3), exhibited clear peaks at around 1.4 V during the cathodic scan and around 2.4 V during the anodic scan. These peaks correspond respectively to the formation of lithium polysulfides and their conversion to elemental sulfur and lithium, i.e. discharge-charge of the battery. The first cycle showed a different behavior with a cathodic peak at around 2.2 V, no well-defined peaks at lower voltage but a higher cathodic current. This peculiar behavior, during the first cycle was also found in the charge-discharge voltage versus capacity curves (Fig. 4). During the first discharge, the battery yielded a capacity of around 3100 $mAhg^{-1}$ of sulfur. This is almost twice the theoretical discharge capacity (1675 $mAhg^{-1}$ for sulfur). Furthermore, a voltage plateau at around 2.4 V was also visible; the difference in voltage with the 2.2 V observed during the cyclic voltammetry is due to the difference in current density used in the two different measurements. During the following cycles the capacity stabilized around the theoretical value and the high voltage plateau faded with the number of cycles. With liquid electrolytes, at

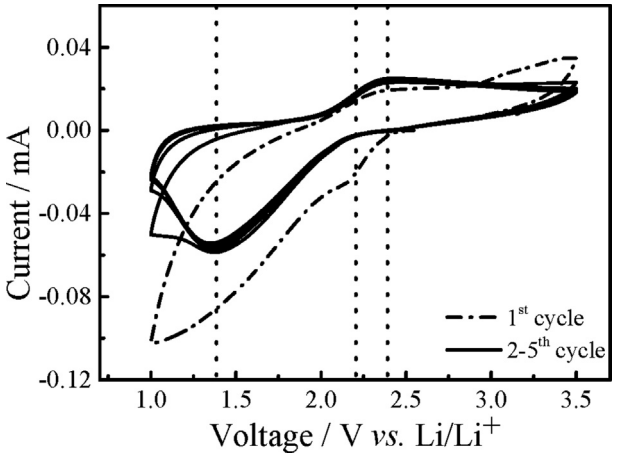

Fig. 3 – Cyclic voltammogram (at 55 °C and scan rate of 0.1 mV s^{-1}) of a solid-state Li|$LiBH_4$@SiO_2|S+C battery based on a $LiBH_4$-SiO_2 nanocomposite electrolyte [17].

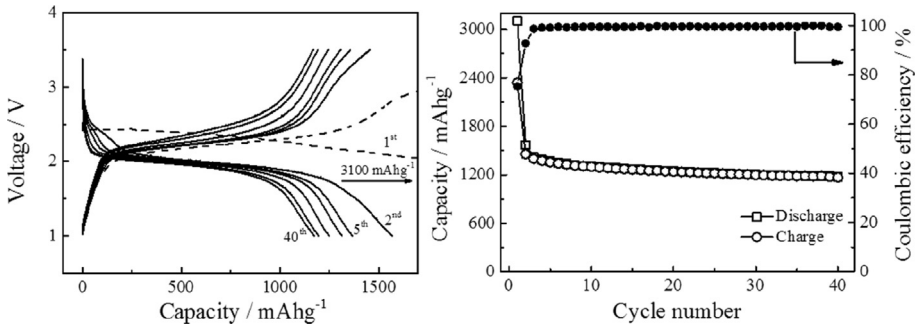

Fig. 4 – Cycling performance and discharge/charge capacity and Coulombic efficiency of a solid-state Li-S battery based on $LiBH_4$-SiO2 nanocomposite as electrolyte, measured at 55 °C, current density of 6.2 μA cm^{-2}, corresponding to C-rates of 0.03 C, and with cut-off voltages of 1 and 3.5 V [17].

least two voltage plateaus must be observed. A first one following the dissolution of the high order polysulfides (Li_2S_8), the discharge occurring in the liquid phase and a second one, with the precipitation of lower order polysulfides (Li_2S_x, $1 \leq x < 8$), the discharge occurring between liquid-solid phases [21]. For solid-state Li-S batteries, only one plateau is expected for the solid-state electrochemical reactions [22]. Therefore, the large capacity obtained during the first cycle together with the fading high voltage plateau were attributed to parasitic electrochemical reactions between the solid electrolyte and the sulfur electrode, possibly forming a stable cathode-electrolyte interface (CEI). The nature of these reactions as well as of the interface is the subject of an ongoing research. Possible reaction of the electrolyte with Li metal was excluded following the galvanostatic plating-stripping studies performed on symmetric cells.

During the 3rd cycle, the capacity stabilized to around 1570 $mAhg^{-1}$ of sulfur, (94% of the theoretical capacity) and gradually decreases to 78% of this value after 40 cycles. The authors attributed the small loss in capacity upon cycling to an increase in the overall resistivity of the cell (from 1.2 kΩ to 1.8 kΩ after the first cycle to about 5 kΩ after the 40th cycle). The increased resistance could arise from the formation of an insulating CEI and partial loss of contact between the electrodes and electrolyte, as observed for other type of solid-state batteries based on lithium borohydride solid-electrolytes [23–25].

The rate capability measurements on the full Li-S at different charge-discharge rates (0.03 C–0.12 C) indicates that the capacities are lower at higher C-rates, but full capacity is regained when the charge rate is lowered again to 0.03 C. The low capacity at high charge-discharge rate is attributed to polarization of the sulfur electrode. At high C-rates, full sulfur utilization is impeded by the large potential drop in the C+S cathode, indeed sulfur and lithium-sulfur compounds have low electronic conductivities; this could be remediated by using more highly conductive carbon additives and improved dispersion of sulfur with smaller particle size. The recovering of the full capacity after lowering the rate underscores the good stability of the solid-state Li-S battery based on $LiBH_4$@SiO_2 nanocomposite as electrolyte. Current effort is devoted to improving the sulfur utilization at high rates via re-engineering of the S+C cathode, to improve electronic conductivity and interfacial contact with the electrolyte during cycling. Further work is devoted in obtaining a better fundamental understanding of the ionic transport in this type of composite solid electrolyte and at the interfaces with the electrodes [26].

$Li|Li(BH_4)_{0.75}I_{0.25}+(Li_2S)_{0.75}(P_2S_5)_{0.25}|TiS_2$

Progress has also been made at the solid electrolyte level by proceeding to the optimization of the composition in the electrolyte system $Li(BH_4)_{0.75}I_{0.25}+Li_2S+P_2S_5$ [27]. Indeed, the highest *RT* ionic conductivity (~10^{-3} S cm^{-1}) was found for the system with the approximate nominal composition $Li(BH_4)_{0.75}I_{0.25}+(Li_2S)_{0.75}+(P_2S_5)_{0.25}$ with an activation energy of 0.30(2) eV. In this approach, it appeared that [BH_4^-] groups are structurally influenced by the presence of [PS_4^{3-}], likely as it does for the [I^-] anions [28]. This allows less hindered effect regarding Li mobility and consequently facilitating the Li ion conduction in the mixed system at lower temperatures *RT*–150 °C. This composite electrolyte seems to show an electrochemical window up to 5 V and stability in contact with Li metal and battery tests using TiS_2 electrodes show notable initial reversibility for further work on advanced battery tests (Fig. 5).

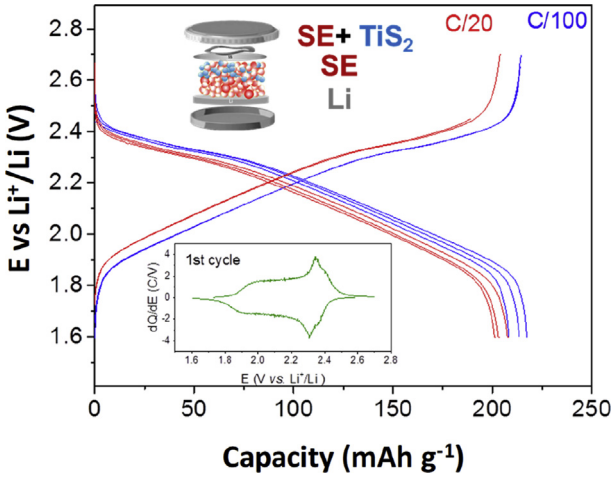

Fig. 5 – Electrochemical galvanostatic discharge/charge cycling with TiS_2 electrode with $Li(BH_4)_{0.75}I_{0.25}+(Li_2S)_{0.75}+(P_2S_5)_{0.25}$ solid electrolyte at 50 °C (Inset: dQ/dE curve for the first cycle) [27].

Noticeably, the cell configuration $TiS_2|Li(BH_4)_{0.75}I_{0.25}+(Li_2S)_{0.75}+(P_2S_5)_{0.25}|Li$ shows a first discharge capacity of 91% of the theoretical one for TiS_2 (~239 mAh.g^{-1}) with reversibility yield of about 98%. The following three discharge curves indicate a good cyclability and optimal coulombic efficiency at two different rates. Primarily, these tests are very promising as it shows repeatable cycling, mainly during the delithiation (superimposed curves) for the experienced cycling rates, meaning good response can be expected at fast recharge solicitation. Secondly, the lithiation emphasizes the good stability of the TiS_2 electrode toward the solid electrolyte with no significant side reaction (inset in Fig. 5) can be observed as the system remains almost fully reversible during cycling for the same current rate.

$Li|LiCB_{11}H_{12}$ or $Li_2B_{12}H_{12}|S$

Recently, beside $LiBH_4$-type electrolytes, other *closo*-type complex hydrides containing so-called *closo*-type (cage-like) complex anions (such as $B_{12}H_{12}^{2-}$, $CB_{11}H_{12}^{-}$, and $CB_9H_{10}^{-}$) have been investigated intensively due to the high ion conductivities approaching 10^{-1} S cm^{-1} in their high-T phases [29–31]. When $LiCB_{11}H_{12}$ was used as solid electrolytes, the all-solid-state Li-TiS_2 battery delivered high initial discharge capacity of ~230 mAhg^{-1} for a rate of 0.2C at 403 K [31], as shown in Fig. 6a. Despite the high initial capacity at a relatively high rate, they exhibited large capacity loss during cycling and the 5th discharging retained only 75% of the initial capacity (Fig. 6a). One possible reason of this poor performance is high reactivity of carbon in complex anions with the lithium metal. It is noted that carbon is the commercial anode material in the conventional liquid-based lithium-ion batteries [32].

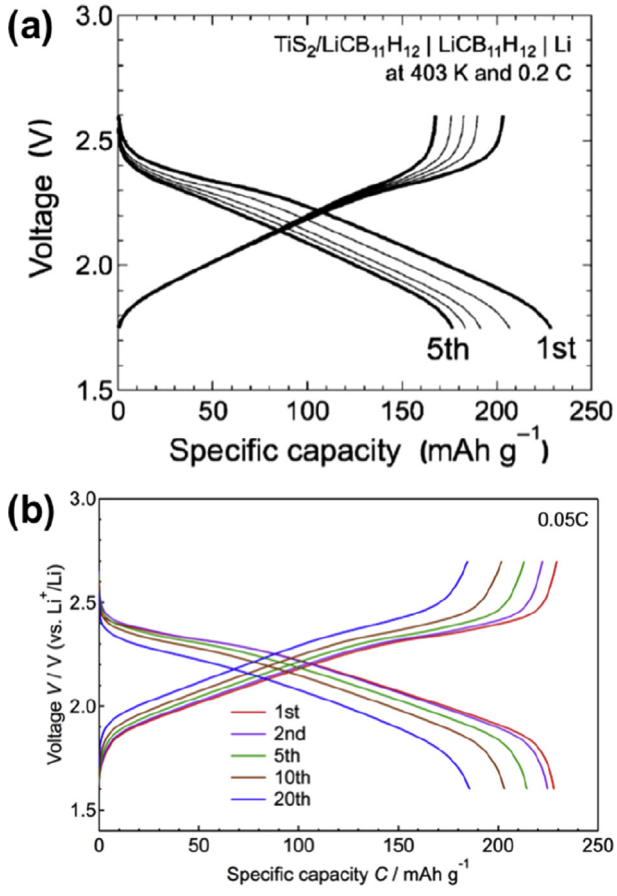

Fig. 6 – All-solid-state batteries using closo-type complex hydride solid electrolytes. Discharge-charge profiles of (a) $Li|LiCB_{11}H_{12}|TiS_2$ [30] and (b) Li|atom-deficient $Li_2B_{12}H_{12}|TiS_2$ batteries [28].

The important feature of *closo*-type complex hydrides that differentiates them from $LiBH_4$-based compounds is that complex anions consist of not only multiple H atoms but also multiple B (and C) atoms. In such *closo*-type complex anions, the B and H atoms form a particular covalent bonding pattern (B–B and B–H), leading to the robust cage-type polyanionic structure. Recent experimental and theoretical study on the basis of the given peculiar structure of *closo*-type complex anions reveals that lithium and hydrogen could be simultaneously extracted from $Li_2B_{12}H_{12}$ by applying a small external energy, enabling the formation of atom-deficient *closo*-type compounds [29]. These atom deficiencies lead to an increase in carrier concentration, improving lithium-ion conductivity by 3 orders of magnitude (2 10^{-5} S cm^{-1} at 30 °C) compared to that of a pristine material (2.5 10^{-8} S cm^{-1} at 30 °C). An all-solid-state Li-TiS_2 battery employing atom-deficient $Li_2B_{12}H_{12}$ as a solid electrolyte exhibited a first discharge capacity of 228 mAhg^{-1} and good capacity retention over 20 cycles for a rate of 0.05C at 353 K (Fig. 6b). These results suggest that atom-deficient *closo*-type materials can be used as the solid electrolyte in all-solid-state batteries.

Full-cell configurations combining metal hydride anode and complex hydride electrolyte

MgH_2-$TiH_2|LiBH_4|S+Li_2S+C$

A metal-hydride (MH; M = Mg, Ti)) nanocomposite made from MgH_2 and TiH_2 counterparts (with 8:2 M ratio) and a complex borohydride solid electrolyte ($LiBH_4$) were integrated in a complete solid-state battery with a sulfur+carbon composite as cathode [33]. $LiBH_4$ was used as the solid electrolyte due to its high Li^+ conductivity of 10^{-3} S cm^{-1} at 120 °C, suitable mechanical properties and outstanding performance in LIBs [6,14,34,35].

The anode electrode was prepared from a mixture of the MH composite with C65 conductive carbon black and $LiBH_4$. The positive electrode was made from a mixture of Li_2S with $LiBH_4$ and carbon Ketjen Black (KB). This mixture was obtained from the first discharge of a $S+LiBH_4+KB|LiBH_4|Li$ half-cell. The redox reaction (Eq. (3)) for the full-cell can be written as:

$$Li_2S + (yMgH_2+(1-y)TiH_2) \rightarrow S + (yMg+(1-y)Ti) + 2LiH \quad (3)$$

With theoretical reduction potentials at 1.7 V and 2.0 V *vs* Li/Li^+, for MgH_2 and TiH_2, respectively, the charge/discharge profiles for the complete cell are shown in Fig. 7. On the first charge, three plateaus are observed: a large sloping first plateau at ~1.8 V, followed by a second smaller one at approx. 2.2 V and an even smaller third one at approx. 2.35 V. The first and second plateaus correspond to the conversion reaction of MgH_2 and TiH_2 phases with lithium, respectively. The third plateau at ~2.35 V is attributed to minor lithiation of Mg metal. The reached capacity (1720 mAhg^{-1}) suggests the complete lithiation of the metal hydride mixture.

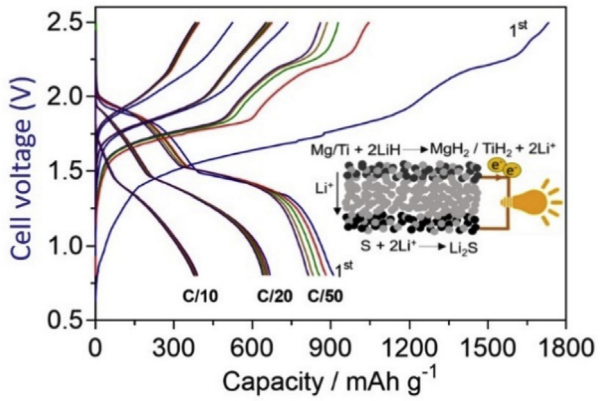

Fig. 7 – Charge/discharge profiles at different C rates (C/50, C/20 and C/10, five cycles each) of the complete ASS battery Li_2S+$LiBH_4$+KB|$LiBH_4$|MH+$LiBH_4$+C65 at 120°C and schematic representation of the discharge redox reaction [33].

First discharge of the complete cell exhibits two plateaus at 1.8 and 1.4 V corresponding to the reformation of TiH_2 and MgH_2, respectively. The cell shows an excellent outcome, with reversible capacities as high as 910 $mAhg^{-1}$ at C/50. The capacity of the battery gradually decreases with increasing the C rate due to kinetic constraints of the MH redox conversion. Despite this, the capacity was successfully recovered to *ca.* 780 $mAhg^{-1}$ at C/50 after 20 cycles (Fig. 8). Coulombic efficiency remained over 97% after the initial cycles.

The present work comes out from the smart concept of merging for the first time in a complete all-solid-state cell, a high-performance nanocomposite hydride anode with sulfur as cathode. The electrochemical performance of the complete cell demonstrates the potential of metal hydrides for high-energy all-solid-state Li batteries.

Operando study of Li cell by neutron diffraction

In-situ and *operando* studies of working electrodes have been developed by several groups in the past using either conventional lab or SR X-ray radiations both for diffraction or absorption [8,9,27,36–38], leading to valuable results for comprehension of the electrochemical reaction mechanisms. This was mainly done with half-cells using specially designed devices like the electrochemical cell of Leriche et al. dedicated to *operando* studies [39]. However, such devices are not well designed for bulk analysis as X-ray beam can hardly go through matter containing metallic elements because of strong absorption. This impedes bulk analysis of full-cells as the crossing all the components (casing, current collectors, electrodes, electrolyte, separators…) is not easily achievable. To overcome these difficulties, use of neutron beam is very interesting as it can penetrate deeply in materials without significant absorption for most of the elements. In addition, with the high hydrogen content it will appear a heavy background due to large incoherent scattering. This last point can be solved by using deuterium instead of hydrogen or by limiting the hydrogen content in the cell.

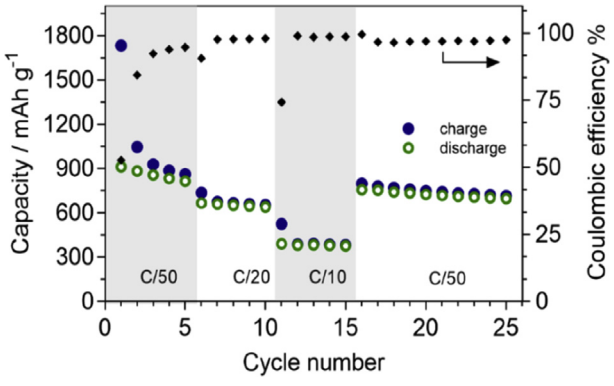

Fig. 8 – Charge/discharge profiles at different C rates (C/50, C/20 and C/10 then C/50 again, five cycles each) of the complete solid-state battery Li_2S+$LiBH_4$+KB|$LiBH_4$|MH+$LiBH_4$+C65 at 120 °C [35].

Recently, we used neutrons as an efficient probe for Li-ion batteries to investigate the structural evolution of the electrode materials in an ICR 10440 commercial cylindrical cell shown in Fig. S1 of the Supplementary Information file (A3 type rechargeable battery with a diameter of 10 mm and length of 45 mm; capacity 360 mAh; operating voltage 3.7 V [40]).

The battery showed a practical capacity of 360 mAh operating at 3.7 V [40]. The multicomponent cathode material was identified as a combination of three phases: $Li(Ni,Mn,Co)O_2$, $LiCoO_2$ and $LiMn_2O_4$ whereas the anode was made of commonly used graphite. The high neutron flux of 10^{14} n cm^{-2} s^{-1} available at SINQ, PSI, allows studies of the transformation processes at a relatively short time scale. Importantly, neutron scattering is interacting with nuclei of the elements and is thus independent of the atomic number of the elements and allows studies of both atomic structures and macroscopic characterization of Li distribution in the studied batteries as related to their state of charge, rate of battery charge and discharge and temperature of the system studied. In the present study, accumulated high quality neutron diffraction data sets collected in just 3–5 min were suitable to accomplish Rietveld refinements.

Upon cycling, the data analysis showed that graphite underwent structural changes to form a various insertion-type lithiated LiC_x, with a maximum volume expansion of 12.7% for the compound LiC_6. For the cathode, the charge process was related to fractional lithium depletion from the Li-saturated compounds, leading to a small volume contraction for the layered oxides. Successful Rietveld fitting of the diffraction pattern allowed identification of all individual constituents and showed that there were as many as 7 components accounted during the refinement (Fig. 9).

Upon cycling, the data analysis showed that graphite underwent structural changes to form a various insertion-type lithiated LiC_x, leading to 12.7% volume expansion for the compound LiC_6. For the cathode, the charge process was related to fractional lithium depletion from the Li-saturated compounds, leading to volume contraction for $Li(Ni,Mn,Co)O_2$, in contrast to (Ni,Mn)-free $LiCoO_2$. For the discharge completed at fast rate (2C) for various temperatures (5, 25 and 45 °C), the capacity followed the trend of an increased diffusion rate of Li^+ in the electrolyte and Li in the two electrodes,

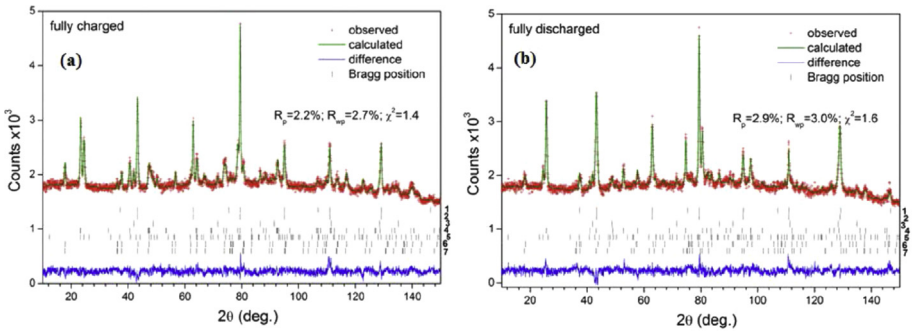

Fig. 9 – Neutron diffraction patterns for the fully charged (a) and discharged (b) battery along with the results of the Rietveld refinements. Phase constituents, from bottom to top: (a) $Li_{0.2}(Ni,Mn,Co)O_2$, $Li_{0.4}CoO_2$, LiC_{12}, LiC_6, Cu, Fe, Al; (b) $Li(Ni,Mn,Co)O_2$, $LiCoO_2$, LiC_{12}, C, Cu, Fe, Al.

especially at 45 °C. Successful refinement of the diffraction patterns requires identification of all individual constituents which contribute to the scattering of the diffraction beam. Together with constituents of the cathode, anode, the material of the current collectors and casing should be properly accounted to quantitatively assess the phase-structure transformations taking place. Fig. 9 shows that there were as many as 7 components accounted during the Rietveld refinement of the data.

Further to neutron diffraction, conventional neutron radiography is an excellent way of imaging various types of battery cells, where the high penetration of neutrons appears to be extremely useful for imaging a battery interior during *in-situ* studies. Experiments with ICR 10440 battery cell were performed at ICON cold neutron imaging facility at SIN, PSI and some results are shown in Fig. 10 [41] and show variations of lithium content as related to the state of the battery.

During operation, swelling and contraction of the active material on cycling was manifested by change of the level of electrolyte as related to the state of charge (0, 50 and 100%; Fig. S2).

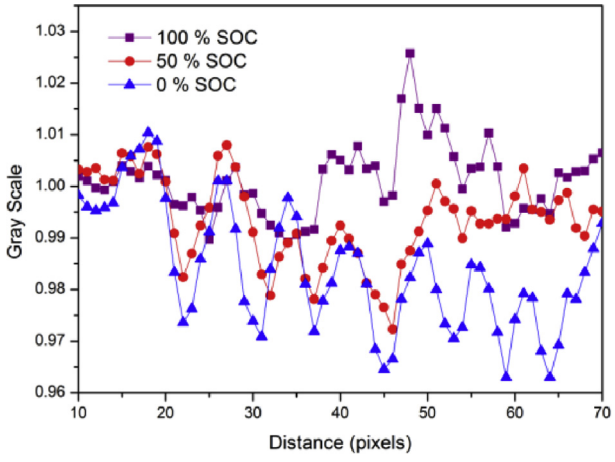

Fig. 10 – Change in contrast as related to the state of charge of the battery within the yellow marked area (right image) which are caused by the change in lithium content. (For interpretation of the references to color in this figure legend, the reader is referred to the Web version of this article.)

This work demonstrates that *operando* and *in-situ* neutron scattering studies of a full-cell battery lead to a valuable information on the complex mechanisms involved upon cycling, related to structural changes in the anode and cathode materials. Moreover, in the frame of this paper, it might also bring new insights on the solid electrolyte, if any structural changes occur (as it is typically the case for $LiBH_4$ for which superionic properties can be followed through the structural transition observed only for the hexagonal high temperature modification of the complex hydride).

Discussion

Recently, metal hydrides have been successfully used as electrodes in half-cell solid state configurations using solid $LiBH_4$ and Li_2S+P_2S_5 electrolytes [42–46]. In some cases, these have proved to be superior to their liquid-electrolyte counterparts. A solid-state battery $MgH_2|LiBH_4|Li$ has been demonstrated in Li-ion half-cell configuration by Kojima and co-workers where lithium metal was used as auxiliary/reference electrode [46]. The active material was prepared by mixing MgH_2 and $LiBH_4$ (2:1 wt ratio). In addition to carbon black additive, the MgH_2 anode was doped with Nb_2O_5 (1 mol.%) to improve the electrochemical performance [43]. This hydride-optimized half-cell yielded high reversible capacity (1586 $mAhg^{-1}$) with low polarization of 0.05 V. Unfortunately, the capacity retention decreased significantly to 924 $mAhg^{-1}$ within 50 cycles. Possible formation of $Mg(BH_4)_2$, because of interaction of MgH_2 with $LiBH_4$, may occur at higher voltage (2 V). Besides, similarly to the alloying mechanism happening in carbonate-based liquid electrolytes at low voltage [47], the formation of Mg-Li alloys may occur also in solid-state configuration. This both unwanted processes, happening at extreme compositions, can be avoided by limiting the voltage to 0.3–1 V [46]. The reversible capacity (~1200 $mAh.g^{-1}$) of the $MgH_2|LiBH_4|Li$ cell has been improved using carbon nanofiber-supported MgH_2 composite electrode, thanks to the enhancement in the electronic conductivity of MgH_2 [45]. Rate capability tests showed a capacity retention of 1100 $mAhg^{-1}$ at high current density (4C rate). Different cells configurations were assembled by incorporating an additional layer of $80Li_2S$+$20P_2S_5$ solid electrolyte (Li side) for possible use in full cells. Comparable performance between cells with

Table 1 – Half- and full-cell systems developed with metallic and/or complex hydrides as electrode or electrolyte. Works done by the IEA-Task 32 partners are highlighted in grey (CE: Coulombic Efficiency; AC: Activated Carbon; VGCF: Vapor Grown Carbon nanoFibers; KB: Ketjen Black; PVDF: PolyVinyliDene Fluoride).

Cell type	Active material	Conductor/ Binder	Electrolyte	Counter electrode	E^- (V)	E^+ (V)	Current density	Rate	T (°C)	1st disch. ($mAhg^{-1}$)	Reversibility ($mAhg^{-1}$)	Cycling (Cyc.)	CE (%)	Reference
Half-	TiH_2	AC 30	$LiBH_4$	Li	0.05	1	400 mAg^{-1}	C/4	120	1052	878	50	86	[44]
Half-	MgH_2 (Nb_2O_5 1%)	VGCF nanofiber	$80Li_2S$-$20P_2S_5$	Li	0.3	1	200–8000 mAg^{-1}	0.1–4C	120	1382–1731	840	1st	60.8–96.7	[45]
Half-	MgH_2 (Nb_2O_5 1%)	VGCF nanofiber	$80Li_2S$-$20P_2S_5$	Li	0.3	1	200–8000 mAg^{-1}	0.1–4C	120	1214	575	1st	47.3	[45]
Half-	MgH_2 (Nb_2O_5 1%)	AC black	$LiBH_4$	Li	0.3	1	100–3200 mAg^{-1}	–	120	1650	924	50	99.5	[46]
Half-	MgH_2 (CoO 25%)	AC black	$LiBH_4$	Li	0.3	1	–	0.05–0.5C	120	1240	900	20	99	[10]
Half-	MgH_2 (Al_2O_3 5%)	AC black	$80Li_2S$-$20P_2S_5$	Li	0.1	2	0.05 $mAcm^{-2}$	–	100	1171	861	10	52	[42]
Half-	MgH_2	AC + PVDF	$Li(BH_4)_{0.75}I_{0.25} + (Li_2S)_{0.8}(P_2S_5)_{0.2}$	Li	0.2	1.8	10 μAcm^{-2}	–	30	652	550	3	–	[11]
Half-	Mg_2FeH_6	AC MTI Corp.	$LiBH_4$	Li	0.3	1	–	C/50	120	1200	300	10	95	[8]
Full-	TiS_2	none	$Li(BH_4)_{0.75}I_{0.25} + (Li_2S)_{0.75}(P_2S_5)_{0.25}$	Li	1.6	2.7	10 μAcm^{-2}	C/100 C/20	50	239	200	6	96	[11]
Full-	TiS_2	none	$Li(BH_4)_{0.75}I_{0.25} + (Li_2S)_{0.75}(P_2S_5)_{0.25}$	Li-In	1	2.4	114 μAcm^{-2}	C/10	27	228	192	10	99	[59]
Full-	TiS_2	none	$LiBH_4$	Li	1.6	2.7	230 μAcm^{-2}	C/5	120	205	180	300	99	[15]
Full-	TiS_2	none	$LiCB_{11}H_{12}$	Li	1.75	2.6	285 μAcm^{-2}	C/5	130	200	175	5	95	[30]
Full-	TiS_2	none	$Li_2B_{12}H_{12}$	Li	1.6	2.7	239 mAg^{-1}	C/20	80	228	180	20	–	[29]
Full-	Sulfur	KB + AC +PVDF	$LiBH_4$ @ SiO_2	Li	1	3.5	25 μAcm^{-2}	C/33	55	1570	1220	40	99.6	[17]
Full-	Sulfur	Maxsorb + KB	$LiBH_4$	Li	1	2.4	250 μAcm^{-2}	C/20	120	1140	700	45	99	[14]
Full-	Sulfur	Maxsorb + KB	$LiBH_4$ + LiCl	Li	1	2.5	150 μAcm^{-2}	C/33	100	1377	600	5	99	[13]
Full-	Sulfur	KB 600	$LiCe(BH_4)_3Cl$	Li-In	0.6	2.4	13 μAcm^{-2}	C/100	45	870	510	9	73	[51]
Full-	Li_2S/S	C65	$LiBH_4$	MgH_2+TiH_2	0.8	2,5	–	C/50 C/20 C/10	120	910	780	25	97	[35]
Full-	$LiCoO_2$	Li_3PO_4 coating	$LiBH_4$	Li	3	4.2	65–130 μAcm^{-2}	–	120	89	86	30	–	[33]
Full-	$Li_4Ti_5O_{12}$	C65 + PVDF	$Li(BH_4)_{0.81}I_{0.19}$	Li	1	2.6	12.7 μAcm^{-2}	–	60	142	10	200		[25]

and without $80Li_2S+20P_2S_5$ solid electrolyte, were reached in this study [45]. In quite similar cell configuration with $LiBH_4$ solid electrolyte, the *in-situ* incorporation of the highly dispersive CoO/Co nanoparticles to MgH_2 led to improvement of the cyclability and reversibility, and mitigated kinetics at high rate between the charge and discharge. The present results may open up to possibilities for making a bulk-type solid-state full battery with cathode materials such as $LiCoO_2$ [45].

Very recently, a new series of rare earth metal borohydrides, $LiM(BH_4)_3Cl$, M = La, Ce, Gd, were found to have high Li^+ ion conductivity, with $\sigma(Li^+)$ approx. 10^{-4} Scm^{-1} at room temperature [48–50]. The cerium-based compound, $LiCe(BH_4)_3Cl$, exhibits the highest stability when employed in Li and Li-In alloy symmetrical cells without formation of resistive layers upon cycling. This compound, $LiCe(BH_4)_3Cl$, is also demonstrated as an electrolyte in solid-state Li-S batteries using a carbon-sulfur composite as cathode and Li-In as anode. A reversible electrochemical reaction between Li and S with an initial discharge capacity of 1186 $mAhg^{-1}$ and a current density of 13 $\mu A\ cm^{-2}$ (i.e. a rate of charge/discharge of *C*/100) takes place at 45 °C with a remaining capacity of 510 $mAhg^{-1}$ after 9 cycles [51].

The discovery of the electrochemical properties of hydride as conversion anodes or Li-superconductor electrolytes is quite recent, as first published papers on that matter appeared only ten years ago. Nevertheless, much work has been devoted to the characterization of their electrochemical properties in half- or full-cells. Table 1 gathers the results obtained so far for systems combining solid-state electrolytes with various electrode materials including metallic hydrides. It is worth to note in this table that half-cells (using Li as counter electrode) were mainly tested with MgH_2 (using different additives improving electronic conduction, binding or activation). Indeed, the use of MgH_2 as anodes in Li-batteries remains hampered by poor cycling stability [47]. Much effort has been put into improving the cycling properties, e.g. by ball milling with conductive carbon, use of different binders and nanoconfinement in porous carbon [52–55]. Beside MgH_2, two other hydrides (TiH_2 and Mg_2FeH_6) have been also tested with success. Regarding electrolytes, $LiBH_4$-type ones are mainly used and improved with various substitutions (LiI, Li_2S, P_2S_5, …) though other non-hydride systems were also tested (like $80Li_2S+20P_2S_5$). Half-cells were investigated in potential windows between 0.05-0.3 and 1–2 V at T = 120 °C according to the enhanced Li conductivity of the high-temperature $LiBH_4$ phase except for two of them for which a low temperature electrolyte $(Li(BH_4)_{0.75}I_{0.25} + (Li_2S)_{0.75}+(P_2S_5)_{0.25})$ allowed to work close to *RT* (30 °C). All systems give rather high capacities at the first discharge (more than 650 $mAhg^{-1}$) and reversible capacities ranging between 550 and 878 $mAhg^{-1}$ for at least a few tens of cycles with CE ranging between 47 and 99.5%.

Beside half-cells, the most important challenge remains the development of full-cells with enhanced properties compared to the state-of-the-art. Metal and complex hydrides might be used as anode or electrolyte but, for building a full battery, should also be coupled to a suitable positive electrode. Sveinbjornsson et al. [25] have used lithium titanate ($Li_4Ti_5O_{12}$). A significant overvoltage and a sloppy voltage were observed, especially during discharge. The battery showed rapid capacity fading over cycling. Another attempt was made by Takahashi et al. [33] with the classically-used cathode material $LiCoO_2$ but stabilization of the interface between this oxide and the reductive borohydride remains very challenging. Thus, a coating made of Li_3PO_4 was necessary to protect the interface. Sulfur-based materials, though working at lower potential (roughly 2.2 V), were more simply used to build full-cell batteries. Mainly, pure sulfur, Li_2S and TiS_2 were tested successfully. Again, the use of $LiBH_4$ as electrolyte implies a working temperature larger or equal to 120 °C but various strategies (substitution by LiI, LiCl, Li_2S or P_2S_5, nanoconfinement in SiO_2, replacement by *closo*-boranes) has allowed to decrease the temperature down to 100-80 °C and even 55-45 °C, keeping practical capacities and reasonable rates. For batteries using metallic lithium as anode, capacities are given regarding the active materials at the cathode (as Li with 3828 $mAhg^{-1}$ can be considered as quasi-infinite beside the cathode) except for López-Aranguren et *al.* [35] that refer to the composite MgH_2+TiH_2 anode. Thus, comparison is not straightforward though one can notice that full-cells built with TiS_2 are less capacitive than the sulfur ones, because of the extra weight brought by Ti and the lower S/Li ratio. For sulfur, capacities as high as 1140–1570 $mAhg^{-1}$ are reported. Reversible capacities are also significant, ranging from 510 to 1220 $mAhg^{-1}$ with CE from 73% to 99,6% for a few tens of cycles. Finally, it is worth to note that only one full-cell combining both metallic hydride as anode and complex hydride as electrolyte has been reported so far. The system $MgH_2+TiH_2|LiBH_4|S+Li_2S$ can provide more than 720 $mAhg^{-1}$ for at least 25 cycles at 120 °C [35]. It is important to keep in mind that the use or metallic lithium as anode, though very promising due to the very high capacity of Li, remains challenging in terms of safety. Dendrites might find a path within the granular morphology of solid electrolytes leading to hazardous shortcuts. Indeed, recovering of a lithium plate negative electrode upon prolonged cycling is not straightforward and anodic host structures could be mandatory keeping increasing interests in the development of conversion materials like metallic hydrides.

Despite proof of concept for the usability of metallic and complex hydrides as anodes and electrolytes to develop full-cell solid-batteries, some drawbacks remain to be solved to go forward into electrochemical applications. Regarding anodes, the conversion reaction between metallic hydrides and lithium is easily observed as far as $\Delta G_f(MH_x)/x$ is greater than $\Delta G_f(LiH)$. However, the reversibility remains an issue as the recovery of the hydride from the metal and lithium hydride is quite challenging. A recent study has explored how different preparation methods influence the electrochemical reactivity of MgH_2 and what may cause the fast capacity fade [56]. Huen et *al.* [56] found that growth of the Mg crystallites upon discharge may limit the Mg-LiH surface contact and thereby hinder the reversibility, and that part of the Mg formed during discharge can be reconverted into MgH_2 during charge, while the reconverted MgH_2 cannot fully react in subsequent discharge. Thus, the hydride conversion may be hampered by limited diffusion of Mg. The results agree with a kinetically limited process tracked by impedance as function of particle size and state of charge [57]. This issue was also investigated

in a recent work on a MgH_2 thin film [58]. Basing their study on a 2D thin-film electrode, the authors discarded electronic or morphologic degradations but identified mass-transport limitation as the main factor for hampering the reversibility of the conversion reaction. Future strategies should pay attention to the understanding and enhancement of mass-transport of hydrogen, lithium and metal atoms within the solid-state electrode especially at room temperature.

For solid-state electrolytes, the main challenge remains the working temperature that is still too high for practical applications. Though improvement have been made by playing with substitutions in the anion sublattice or nanoconfinement, liquid-like ionic conductivities at room temperature remains difficult to achieve. In addition, electrode formulations are still to be improved to ensure good interfaces between the active materials and the electrolyte keeping practical mechanic properties for the system.

Finally, a lot is still to be understood on the electrochemical reaction paths, the role of interfaces and the ionic conduction mechanisms in solid-state electrolytes. The development of powerful *operando* techniques using either photons or neutrons beams is mandatory to fully describe the behavior of the complex chemistry involved in real batteries.

Conclusion

Much progress has been achieved in fundamental research to understand the properties of metallic or complex hydrides. Their ability to undergo conversion reactions with lithium to function as capacitive anodes or to transport Li ions to perform as efficient super-ionic conductors has been demonstrated by many research groups worldwide. Those efforts have allowed construction of practical batteries showing better and safer electrochemical properties than classic commercial materials. Though still at its beginning, this research opens a new field for solid-state lithium batteries.

Acknowledgments

Part of this research was funded by the European Marie Curie Action under ECOSTORE grant agreement no. 607040, the Villum Foundation (grant no. VKR023453) and the Danish Council for Independent Research (grant no. 4184-00143A and 4181-00462). This work was also financially supported by Research Council of Norway under the program EnergiX, Project no. 244054, LiMBAT - "Metal hydrides for Li-ion battery anodes" and NordForsk and The Nordic Neutron Science Program via the project FunHy (Project no. 81942). Petra de Jongh and Peter Ngene acknowledge support from NWO-ECHO 712.015.005, and the European Union's Horizon 2020 research and innovation program (ERC-2014-CoG No 648991). All authors are thankful to the International Energy Agency; Hydrogen Implementing Agreement, and especially to all the dedicated and IEA-HIA Task-32 Researchers for their inspired and inspirational work.

Appendix A. Supplementary data

Supplementary data to this article can be found online at https://doi.org/10.1016/j.ijhydene.2018.12.200.

REFERENCES

[1] Cuevas F, Joubert J-M, Latroche M, Percheron-Guégan A. Intermetallic compounds as negative electrodes of Ni/MH batteries. Appl Phys A 2001;72:225–38.
[2] Feng F, Geng M, Northwood DO. Electrochemical behaviour of intermetallic-based metal hydrides used in Ni/metal hydride (MH) batteries: a review. Int J Hydrogen Energy 2001;26:725–34.
[3] Notten PHL, Latroche M. Secondary batteries: nickel batteries metal hydride alloys. In: Garche J, editor. Encycl. Electrochem. Power Sources. Amsterdam: Elsevier; 2009. p. 502–21.
[4] Notten PHL. Rechargeable nickel-metal hydride batteries: a successfull new concept. In: Grandjean F, Long GJ, Buschow KHJ, editors. Interstitial Intermet. Alloys. Dordrecht, Boston, London: Kluwer Academic Publishers; 1995. p. 150–94.
[5] de Jongh PE, Blanchard D, Matsuo M, Udovic TJ, Orimo S. Complex hydrides as room-temperature solid electrolytes for rechargeable batteries. Appl Phys A 2016;122:251. https://doi.org/10.1007/s00339-016-9807-2.
[6] Matsuo M, Orimo S. Lithium fast-ionic conduction in complex hydrides: review and prospects. Adv Energy Mater 2011;1:161–72. https://doi.org/10.1002/aenm.201000012.
[7] Sartori S, Cuevas F, Latroche M. Metal hydrides used as negative electrode materials for Li-ion batteries. Appl Phys A 2016;122:135. https://doi.org/10.1007/s00339-016-9674-x.
[8] Huen P, Ravnsbæk DB. All-solid-state lithium batteries – the Mg_2FeH_6-electrode $LiBH_4$-electrolyte system. Electrochem Commun 2018;87:81–5. https://doi.org/10.1016/j.elecom.2018.01.001.
[9] Provost K, Zhang J, Zaidi W, Paul-Boncour V, Bonnet J-P, Cuevas F, et al. XAS and XRD studies of the thermal and Li-driven electrochemical dehydrogenation of nanocrystalline complex hydrides Mg_2MH_x (M=Co, Ni). J Phys Chem C 2014;118:29554–67. https://doi.org/10.1021/jp509255c.
[10] El Kharbachi A, Uesato H, Kawai H, Wenner S, Miyaoka H, Sørby MH, et al. MgH_2–CoO: a conversion-type composite electrode for $LiBH_4$-based all-solid-state lithium ion batteries. RSC Adv 2018;8. https://doi.org/10.1039/C8RA03340D.
[11] El Kharbachi A, Hu Y, Sørby MH, Mæhlen JP, Vullum PE, Fjellvåg H, et al. Reversibility of metal-hydride anodes in all-solid-state lithium secondary battery operating at room temperature. Solid State Ion 2018;317:263–7. https://doi.org/10.1016/j.ssi.2018.01.037.
[12] El Kharbachi A, Andersen HF, Sørby MH, Vullum PE, Mæhlen JP, Hauback BC. Morphology effects in MgH_2 anode for lithium ion batteries. Int J Hydrogen Energy 2017;42:22551–6. https://doi.org/10.1016/j.ijhydene.2017.04.298.
[13] Unemoto A, Chen C, Wang Z, Matsuo M, Ikeshoji T, Orimo S. Pseudo-binary electrolyte, $LiBH_4$–LiCl, for bulk-type all-solid-state lithium-sulfur battery. Nanotechnology 2015;26:254001.
[14] Unemoto A, Yasaku S, Nogami G, Tazawa M, Taniguchi M, Matsuo M, et al. Development of bulk-type all-solid-state lithium-sulfur battery using $LiBH_4$ electrolyte. Appl Phys Lett 2014;105:083901. https://doi.org/10.1063/1.4893666.

[15] Unemoto A, Ikeshoji T, Yasaku S, Matsuo M, Stavila V, Udovic TJ, et al. Stable interface formation between TiS_2 and $LiBH_4$ in bulk-type All-solid-state lithium batteries. Chem Mater 2015;27:5407–16. https://doi.org/10.1021/acs.chemmater.5b02110.

[16] Maekawa H, Matsuo M, Takamura H, Ando M, Noda Y, Karahashi T, et al. Halide-stabilized $LiBH_4$, a room-temperature lithium fast-ion conductor. J Am Chem Soc 2009;131:894–5. https://doi.org/10.1021/ja807392k.

[17] Das S, Ngene P, Norby P, Vegge T, de Jongh PE, Blanchard D. All-solid-state lithium-sulfur battery based on a nanoconfined $LiBH_4$ electrolyte. J Electrochem Soc 2016;163:A2029–34.

[18] Blanchard D, Nale AC, Sveinbjörnsson D, Eggenhuisen TM, Verkuijlen MHW, Suwarno S, et al. Nanoconfined $LiBH_4$ as a fast lithium ion conductor. Adv Funct Mater 2014;25:184–92. https://doi.org/10.1002/adfm.201402538.

[19] Ngene P, Adelhelm P, Beale AM, de Jong KP, de Jongh PE. $LiBH_4$/SBA-15 nanocomposites prepared by melt infiltration under hydrogen pressure: synthesis and hydrogen sorption properties. J Phys Chem C 2010;114:6163–8. https://doi.org/10.1021/jp9065949.

[20] Ji X, Lee KT, Nazar LF. A highly ordered nanostructured carbon-sulphur cathode for lithium-sulphur batteries. Nat Mater 2009;8:500–6. https://doi.org/10.1038/nmat2460.

[21] Zhang SS. Liquid electrolyte lithium/sulfur battery: fundamental chemistry, problems, and solutions. J Power Sources 2013;231:153–62. https://doi.org/10.1016/j.jpowsour.2012.12.102.

[22] Wang J, He Y-S, Yang J. Sulfur-based composite cathode materials for high-energy rechargeable lithium batteries. Adv Mater 2014;27:569–75. https://doi.org/10.1002/adma.201402569.

[23] Kobayashi T, Imade Y, Shishihara D, Homma K, Nagao M, Watanabe R, et al. All solid-state battery with sulfur electrode and thio-LISICON electrolyte. J Power Sources 2008;182:621–5. https://doi.org/10.1016/j.jpowsour.2008.03.030.

[24] Nagao M, Imade Y, Narisawa H, Kobayashi T, Watanabe R, Yokoi T, et al. All-solid-state Li–sulfur batteries with mesoporous electrode and thio-LISICON solid electrolyte. J Power Sources 2013;222:237–42. https://doi.org/10.1016/j.jpowsour.2012.08.041.

[25] Sveinbjörnsson D, Christiansen AS, Viskinde R, Norby P, Vegge T. The $LiBH_4$-LiI solid solution as an electrolyte in an all-solid-state battery. J Electrochem Soc 2014;161:A1432–9.

[26] Lefevr J, Cervini L, Griffin JM, Blanchard D. Lithium conductivity and ions dynamics in $LiBH_4$/SiO_2solid-electrolytes studied by solid-state NMR and quasi elastic neutron scattering and applied in lithium-sulfur batteries. J Phys Chem Part C 2018;122:15264–75. https://doi.org/10.1021/acs.jpcc.8b01507.

[27] El Kharbachi A, Hu Y, Yoshida K, Vajeeston P, Kim S, Sørby MH, et al. Lithium ionic conduction in composites of $Li(BH_4)_{0,75}I_{0,25}$ and amorphous $0.75Li_2S{\cdot}0.25P_2S_5$ for battery applications. Electrochim Acta 2018;278:332–9. https://doi.org/10.1016/j.electacta.2018.05.041.

[28] Miyazaki R, Karahashi T, Kumatani N, Noda Y, Ando M, Takamura H, et al. Room temperature lithium fast-ion conduction and phase relationship of LiI stabilized $LiBH_4$. Proc 17th Int Conf Solid State Ion 2011;192:143–7. https://doi.org/10.1016/j.ssi.2010.05.017.

[29] Kim S, Toyama N, Oguchi H, Sato T, Takagi S, Ikeshoji T, et al. Fast lithium-ion conduction in atom-deficient *closo*-type complex hydride solid electrolytes. Chem Mater 2018;30:386–91. https://doi.org/10.1021/acs.chemmater.7b03986.

[30] Tang WS, Matsuo M, Wu H, Stavila V, Zhou W, Talin AA, et al. Liquid-like ionic conduction in solid lithium and sodium monocarba-*closo*-decaborates near or at room temperature. Adv Energy Mater 2016;6:1502237. https://doi.org/10.1002/aenm.201502237.

[31] Tang WS, Unemoto A, Zhou W, Stavila V, Matsuo M, Wu H, et al. Unparalleled lithium and sodium superionic conduction in solid electrolytes with large monovalent cage-like anions. Energy Environ Sci 2015;8:3637–45. https://doi.org/10.1039/C5EE02941D.

[32] Tarascon J-M, Armand M. Issues and challenges facing rechargeable lithium batteries. Nature 2001;414:359–67.

[33] López-Aranguren P, Berti N, Dao HA, Zhang J, Cuevas F, Latroche M, et al. An all-solid-state metal hydride – sulfur lithium-ion battery. J Power Sources 2017;357:56–60. https://doi.org/10.1016/j.jpowsour.2017.04.088.

[34] Takahashi K, Hattori K, Yamazaki T, Takada K, Matsuo M, Orimo S, et al. All-solid-state lithium battery with $LiBH_4$ solid electrolyte. J Power Sources 2013;226:61–4. https://doi.org/10.1016/j.jpowsour.2012.10.079.

[35] Unemoto A, Matsuo M, Orimo S -i. Complex hydrides for electrochemical energy storage. Adv Funct Mater 2014;24:2267–79.

[36] Zaïdi W, Bonnet J-P, Zhang J, Cuevas F, Latroche M, Couillaud S, et al. Reactivity of complex hydrides Mg_2FeH_6, Mg_2CoH_5 and Mg_2NiH_4 with lithium ion: far from equilibrium electrochemically driven conversion reactions. Int J Hydrogen Energy 2013;38:4798–808. https://doi.org/10.1016/j.ijhydene.2013.01.157.

[37] Zhang J, Zaïdi W, Paul-Boncour V, Provost K, Michalowicz A, Cuevas F, et al. XAS investigations on nanocrystalline Mg_2FeH_6 used as negative electrode of Li-ion batteries. J Mater Chem A 2013;1:4706.

[38] Teprovich JA, Zhang J, Colon-Mercado H, Cuevas F, Peters B, et al. Li-driven electrochemical conversion reaction of AlH_3, $LiAlH_4$, and $NaAlH_4$. J Phys Chem C 2015;119:4666–74. https://doi.org/10.1021/jp5129595.

[39] Leriche JB, Hamelet S, Shu J, Morcrette M, Masquelier C, Ouvrard G, et al. An electrochemical cell for operando study of lithium batteries using synchrotron radiation. J Electrochem Soc 2010;157:A606–10.

[40] Nazer NS, Yartys VA, Azib T, Latroche M, Cuevas F, Forseth S, et al. In operando neutron diffraction study of a commercial graphite/(Ni, Mn, Co) oxide-based multi-component lithium ion battery. J Power Sources 2016;326:93–103. https://doi.org/10.1016/j.jpowsour.2016.06.105.

[41] Nazer NS, Strobl M, Vie PJS, Yartys VA. In operando neutron radiography investigation of a commercial Li-ion battery at variable current densities. J Power Sources 2018. in preparation.

[42] Ikeda S, Ichikawa T, Goshome K, Yamaguchi S, Miyaoka H, Kojima Y. Anode properties of Al_2O_2-added MgH_2 for all-solid-state lithium-ion batteries. J Solid State Electrochem 2015:1–6. https://doi.org/10.1007/s10008-015-2959-8.

[43] Ikeda S, Ichikawa T, Kawahito K, Hirabayashi K, Miyaoka H, Kojima Y. Anode properties of magnesium hydride catalyzed with niobium oxide for an all solid-state lithium-ion battery. Chem Commun. 2013;49:7174–6. https://doi.org/10.1039/c3cc43987a.

[44] Kawahito K, Zeng L, Ichikawa T, Miyaoka H, Kojima Y. Electrochemical performance of titanium hydride for bulk-type All-solid-state lithium-ion batteries. Mater Trans 2016;57:755–7. https://doi.org/10.2320/matertrans.M2016024.

[45] Zeng L, Ichikawa T, Kawahito K, Miyaoka H, Kojima Y. Bulk-type All-solid-state lithium-ion batteries: remarkable performances of a carbon nanofiber-supported MgH_2

composite electrode. ACS Appl Mater Interfaces 2017;9:2261–6. https://doi.org/10.1021/acsami.6b11314.
[46] Zeng L, Kawahito K, Ikeda S, Ichikawa T, Miyaoka H, Kojima Y. Metal hydride-based materials towards high performance negative electrodes for all-solid-state lithium-ion batteries. Chem Commun. 2015;51:9773–6. https://doi.org/10.1039/C5CC02614H.
[47] Oumellal Y, Rougier A, Nazri GA, Tarascon J-M, Aymard L. Metal hydrides for lithium-ion batteries. Nat Mater 2008;7:916–21.
[48] Ley MB, Boulineau S, Janot R, Filinchuk Y, Jensen TR. New Li ion conductors and solid state hydrogen storage materials: $LiM(BH_4)_3Cl$, M = La, Gd. J Phys Chem C 2012;116:21267–76. https://doi.org/10.1021/jp307762g.
[49] Ley MB, Ravnsbæk DB, Filinchuk Y, Lee Y-S, Janot R, Cho YW, et al. $LiCe(BH_4)_3Cl$, a new lithium-ion conductor and hydrogen storage material with isolated tetranuclear anionic clusters. Chem Mater 2012;24:1654–63. https://doi.org/10.1021/cm300792t.
[50] Payandeh GharibDoust S, Brighi M, Sadikin Y, Ravnsbæk DB, Černý R, Skibsted J, et al. Synthesis, structure, and Li-ion conductivity of $LiLa(BH_4)_3X$, X = Cl, Br, I. J Phys Chem C 2017;121:19010–21. https://doi.org/10.1021/acs.jpcc.7b04905.
[51] Nguyen J, Fleutot B, Janot R. Investigation of the stability of metal borohydrides-based compounds $LiM(BH_4)_3Cl$ (M=La, Ce, Gd) as solid electrolytes for Li-S batteries. Solid State Ion 2018;315:26–32. https://doi.org/10.1016/j.ssi.2017.11.033.
[52] Aymard L, Oumellal Y, Bonnet J-P. Metal hydrides: an innovative and challenging conversion reaction anode for lithium-ion batteries. Beilstein J Nanotechnol 2015;6:1821–39. https://doi.org/10.3762/bjnano.6.186.
[53] Brutti S, Mulas G, Piciollo E, Panero S, Reale P. Magnesium hydride as a high capacity negative electrode for lithium ion batteries. J Mater Chem 2012;22:14531–7. https://doi.org/10.1039/C2JM31827J.
[54] Oumellal Y, Zlotea C, Bastide S, Cachet-Vivier C, Leonel E, Sengmany S, et al. Bottom-up preparation of MgH_2 nanoparticles with enhanced cycle life stability during electrochemical conversion in Li-ion batteries. Nanoscale 2014;6:14459–66. https://doi.org/10.1039/C4NR03444A.
[55] Zaïdi W, Oumellal Y, Bonnet J-P, Zhang J, Cuevas F, Latroche M, et al. Carboxymethylcellulose and carboxymethylcellulose-formate as binders in MgH_2-carbon composites negative electrode for lithium-ion batteries. J Power Sources 2011;196:2854–7.
[56] Huen P, Ravnsbæk DB. Insight into poor cycling stability of MgH_2 anodes. J Electrochem Soc 2017;164:A3138–43.
[57] El Kharbachi A, Hu Y, Sørby MH, Vullum PE, Mæhlen JP, Fjellvåg H, et al. Understanding capacity fading of MgH_2 conversion-type Anodes via structural morphology changes and electrochemical impedance. J Phys Chem C 2018;122:8750–9. https://doi.org/10.1021/acs.jpcc.7b12656.
[58] Berti N, Hadjixenophontosb E, Cuevas F, Zhang J, Lacoste A, Dubot P, et al. Thin films as model system for understanding the electrochemical reaction mechanisms in conversion reaction of MgH_2 with lithium. J Power Sources 2018;402:99–106. https://doi.org/10.1016/j.jpowsour.2018.09.033.
[59] Unemoto A, Wu H, Udovic TJ, Matsuo M, Ikeshoji T, Orimo S, et al. Fast lithium-ionic conduction in a new complex hydride–sulphide crystalline phase. Chem Commun 2016;52:564–6. https://doi.org/10.1039/C5CC07793A.